Available online at www.sciencedirect.com
ScienceDirect
Energy Reports 6 (2020) 358–363
www.elsevier.com/locate/egyr

6th International Conference on Energy and Environment Research, ICEER 2019, 22–25 July, University of Aveiro, Portugal

Introducing Tesla turbine to enhance energy efficiency of refrigeration cycle

Yahya Sheikhnejad*, João Simões, Nelson Martins

Department of Mechanical Engineering & Centre for Mechanical Technology and Automation, University of Aveiro, 3810-193 Aveiro, Portugal

Received 31 July 2019; accepted 30 August 2019

Abstract

In this study, a new application of a Tesla turbine (TT) is presented in which a TT is introduced as a promising solution to enhance the energy efficiency of refrigeration cycles. For this special purpose, a TT is represented as a regenerative system that minimizes the wasted energy without compromising the system output quality or sacrificing standards of design and move one step forward, towards more sustainable industries. To achieve this goal, a 3D thermohydrodynamic analysis of the Newtonian turbulent compressible flow of high-pressure methane through a Tesla turbine has been performed under different configurations and operational conditions. Methane was defined as a real gas through the Redlich–Kwong equation of state. The complex unstructured grid generation was employed to produce a low-skewness mesh for a CFD model on the commercial software of ANSYS Fluent for simulation of heat and mass transfer by FVM. As a result of the present study, practical design rules are proposed to support engineers defining optimized TTs for predetermined operating conditions, namely regarding power output, disc sizes and angular velocity.

Keywords: Energy efficiency; Tesla turbine (TT); Compressible turbulent flow; High-pressure methane; Refrigeration cycles

1. Introduction

According to extensive precise research and measurements all over the world, some bitter facts namely destructive effect of CFC and greenhouse gas (GHG) on ozone depletion and global warming respectively as well as pollution and fast rate of depletion of fossil fuel resources, have been emerged recently which influenced the entire activity of human being in developing and industrial countries. Then, we have had global consensus on this point that with the current rate of GHG emission and pollution production and by having a customary traditional source of energy, the next generation will be vulnerable to various serious dangers and harsh conditions. Consequently, this consensus leads to a new roadmap to change the world progress direction into the sustainable developments [1]. As a part

* Corresponding author.
E-mail address: yahya@ua.pt (Y. Sheikhnejad).

https://doi.org/10.1016/j.egyr.2019.08.073

of researcher's mission to step onto this roadmap, this study tackles one of the most important sources of wasted energy which has been occurred in refrigeration cycles where high-pressure refrigerant from condenser unit must reduce its pressure and be ready for evaporator unit. This procedure usually happen by a throttling valve, capillary tube or expansion valve. This study proposes Tesla turbine as one of the best candidates to be substituted by these wasting devices in order to enhance the coefficient of performance (COP) and reduce wasted energy as well.

Although before 2006 TT was not commercially employed in the industry [2], literature provides a good variety of applications for the TT from solar Rankine cycle combined heat and power systems for small-scale applications [3] to organic Rankine cycle for the low-grade energy utilization [4–6]. In the most recent work, Zhou et al. [7] mentioned the application of the Tesla turbine in engine waste heat recovery and seeking for optimal parameters and geometric model.

Rice [8,9] also provided a brilliant experimental–analytical study which soon have become a benchmark work for unconventional turbomachinery employing a rotor composed of smooth discs, known as TT. Other publications tried to optimize TT [10,11] and draw an outline of TT design rules in laminar incompressible fluid [12].

2. Numerical procedure

A conventional CFD modelling and simulation procedure was followed. The successive major steps of the implemented methodology in this study are as follow. The procedure starts by defining the dimension of TT geometry and generates 3D CAD file in the ANSYS to produce a coherent mesh and after grid dependency test, application of boundary condition and defining methodology, numerical results would be obtained. The procedure was well described in [13–20].

2.1. Grid dependency test

In order to find a relatively optimum grid size such that not only leads to a reliable result but also does not impose a lot of computational costs, grid dependency test was accomplished. By reducing element size, computational cost increases with exponential rate and consequently, mesh rendering and numerical procedure were not performed in a reasonable time. Since the results generated for the grid dependency test did not converge in a region where it would be reasonable for the user to perform a parametric study, the Richardson extrapolation method was used to predict the real result and then an error was applied to this real value and an element size will be determined from that error. The element size that was used, is 5.8e−4 m.

2.2. Grid generations

Finally, after finding an optimum mesh size, the unstructured grid with quadratic element order and two layers of inflations for five discs ($r_o = 50$ mm & b = 1 mm) was generated, Fig. 1. Table 1 provides mesh statistics and quality for the final presented mesh, Fig. 1, which shows that generated mesh has a good quality with low averaged skewness.

Table 1. Statistics and quality of the generated mesh.

Maximum skewness	Average skewness	Number of nodes	Number of elements
0.890	0.343	5,947,910	3,642,217

2.3. Boundary condition

Boundaries in the complicated geometry of TT must be defined at all solid surfaces, inlet port and discharge gate. For both the inlet and outlet sections, a fixed static pressure (respectively 60 and 30 bar) were set and no-slip condition was applied to all solid surfaces. The discs were defined as moving walls rotating over the rotor axis at N rpm. All surfaces of the rotating discs are considered adiabatic and the outer surface of the stator is subjected to free convection. A heat transfer coefficient of 2 W/m^2 K and 15 °C for the environment temperature were assumed.

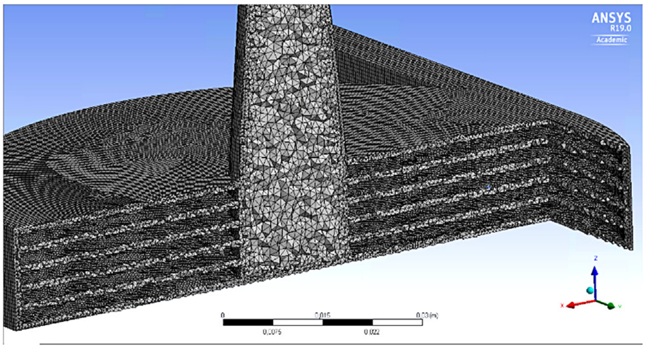

Fig. 1. Unstructured generated mesh for 3D geometry of Tesla turbine.

2.4. Methodology and properties

The SIMPLEC algorithm was adopted as a semi-implicit iterative numerical process in which SIMPLE algorithm is modified to improve convergence in cases where the pressure-velocity coupling is a bottleneck in obtaining a solution. In addition, the value of 0.001 was adopted as the residual convergence criteria for continuity, momentum, turbulent kinetic energy and turbulent dissipation rate but for energy equation, 10–6 was considered. Table 2 describes the values which were considered as under-relaxation factors for different equations. Moreover, the second-order upwind scheme was employed as a spatial discretization method for pressure, momentum, energy, turbulent kinetic energy and turbulent dissipation rate. Only for density, first-order upwind was selected.

Table 2. Values of under-relaxation factors.

Pressure	Density	Momentum	Energy	Turbulent kinetic	Turbulent dissipation
0.3	0.9	0.7	0.9	0.7	0.7

In addition, in order to maintain the accuracy of the result, this investigation tries not to simplify the problem and instead employed the model of high precision and closer to the real condition. Hence, as methane was adopted as a carrier fluid, the Redlich–Kwong equation was used for modelling of real gas density, which is generally more accurate than the van der Waals and the ideal gas equation of state especially at temperatures above the critical temperature. Other properties such as viscosity and specific heat were kept constant. Both these properties change with pressure are dispensable and therefore can be ignored. The fluid properties are summarized in Table 3.

Table 3. properties of carrier fluid.

Property	Value
Density	Real Gas, Redlich–Kwong model
Viscosity	1.087e−5 [kg/m s]
Specific heat capacity	2222 [J/kg K]
Thermal conductivity	0.0332 [W/m K]
Specific heat ratio	1.32

3. Result and discussion

The legend of figures is presented in the RxBx format where Rx refers to the disc outer radius value in millimetres and Bx refers to the disc gap value in millimetres. For example, R75B0.5 refers to a simulation where the disc gap is 0.5 mm and the outer radius is 75 mm. The RxBx format might be used to refer to as a TT geometry or a series of tests where ro and b are kept constant. With ANSYS Fluent it is possible to visualize a certain property of the flow across lines or planes. In order to get a better grasp of what is happening inside the turbine two planes were defined. First, an XY plane parallel to the disc's surface that is located in the middle of the gap of the second and third discs, this plane permits a clear visualization of the flow in between the discs. The second plane is a ZY plane that contains the TT axis and is normal to the inlet which displays well the flow in the outlet.

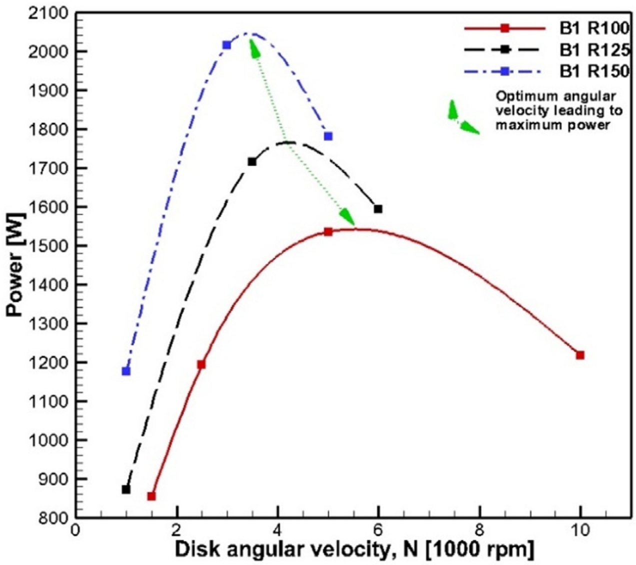

Fig. 2. The generated power variation with disc angular velocity in different TT dimension.

The thermodynamic analysis of TT is begun with generated power by TT in different disc angular velocity and with different disc dimension. As is depicted in Fig. 2, TT shows a non-monotonic characteristic on the variation of generated power with disc rotational speed. The generated power characteristic curve displays a negative curvature which implies a curve having a maximum. It means there is a specific rotational speed, which is so-called "optimum speed", at which TT generated power becomes maximum. Li et al. [21] also reported the same characteristic for the efficiency of TT running with an incompressible carrier fluid in his experimental study. This optimum speed is not fixed but depends on TT dimension (disc diameter) such that optimum speed decreases by increasing disc diameter.

In addition, the magnitude of maximum power corresponding to optimum speed varies by TT dimension such that the magnitude of maximum power will increase by increasing disc diameter. This fact needs to be considered as a design rule for TT. For the configuration of B1R150 the generated power exceeds 2000 W while for the small TT B1R150 it goes up to 1500 W. Moreover, the gradient of characteristic curve of generated power for bigger TT is higher which means generated power will decrease faster for bigger TT by changing disc angular velocity while for smaller TT this variation will be slower and with lower gradient. The outlet temperature is another important dependent variable that its variation versus disc angular velocity is illustrated in Fig. 3. As can be seen, in the limited interval velocity, outlet temperature shows a monotonic increasing behaviour such that in higher rotational speed, characteristic temperature curve shows steeper variations. Moreover, smaller TT has higher outlet temperature than the bigger ones.

Finally, the mass flow rate variation with disc angular velocity is displayed in Fig. 4. In the limited interval of rotational velocity, the TT mass flow rate shows monotonically decreasing behaviour. This phenomenon is due to the centrifugal force, which is proportional to squared rotational speed and opposes against mass transfer towards centre of the disc. In addition, at the same rotational speed, the larger TT shows a higher mass flow rate.

4. Conclusion

By stepping onto the 2030 agenda roadmap and aligned with the objectives of circular economy towards reduction of wastes energy and enhancement of coefficient of performance in refrigeration cycles, this work introduced Tesla turbine as one of the best alternative to reduce refrigerant pressure before entering evaporator unit without compromising the system output quality or sacrificing standards of design. In this work, as a support of above mentioned claim, the thermo-hydrodynamic analysis of compressible high-pressure methane (R50) flow in turbulent regime was performed showing that TT can be capable of producing up to 2 kW (1440 kWh per month, in a 24/7

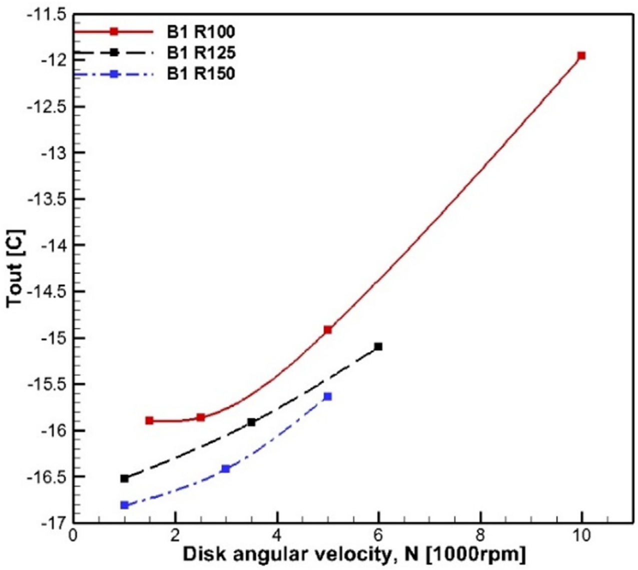

Fig. 3. The outlet temperature variation with disc angular velocity in different TT dimension.

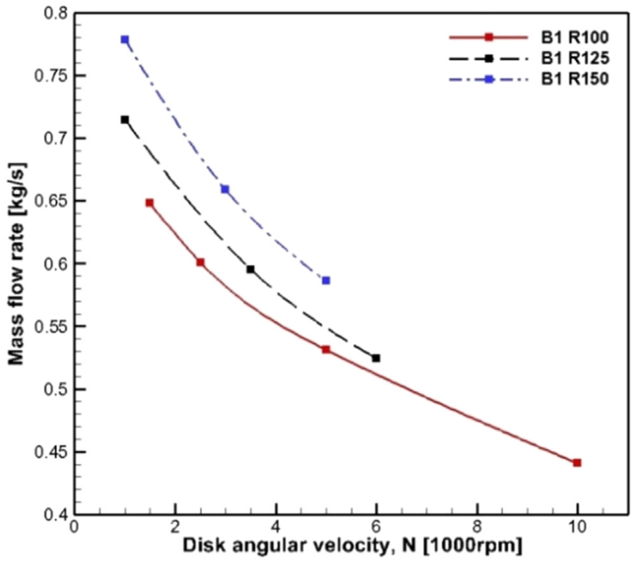

Fig. 4. The mass flow rate variation with disc angular velocity in different TT dimension.

operation basis) in low angular velocity with R150B1 configuration, while working between input–output pressure of 60 and 30 bar. This amount of energy is equivalent to 76 m^2 of monocrystalline silicon photovoltaic solar panel (available commercial PV cell-150 W, 15.4% efficiency and Porto climate condition) working at its maximum power in full sun hours and, enough to light up 285 LED light bulb (7 W) [or 166 (12 W)] simultaneously. This potential, which can be significant in many real cases, has been already wasted in expansion/throttling valves in all industries possessing refrigeration cycle. Considering averaged 40 lumens per square foot for a typical factory, this number of LEDs is enough for lighting of 540 m^2 area. Commercialization of this proposal will have a considerable socio-economic impact and will make our industries more productive and efficient.

Acknowledgements

Acknowledgement to the support of TEMA research unit integrated projects UID/EMS/00481/2013-FCT and CENTRO-01-0145-FEDER-022083.

References

[1] United Nation (UN), n.d. Sustainable Development Goals [WWW Document]. URL https://www.un.org/sustainabledevelopment/sustainable-development-goals/.
[2] Podergajs M. The tesla turbine. Univ. Ljubljana; 2011, p. 1–15.
[3] Carey VP. Assessment of tesla turbine performance for small scale rankine combined heat and power systems. J Eng Gas Turbines Power 2010;132. 122301. http://dx.doi.org/10.1115/1.4001356.
[4] Freeman J, Guarracino I, Kalogirou SA, Markides CN. A small-scale solar organic Rankine cycle combined heat and power system with integrated thermal energy storage. Appl Therm Eng 2017;127:1543–54. http://dx.doi.org/10.1016/j.applthermaleng.2017.07.163.
[5] Manfrida G, Pacini L, Talluri L. A revised Tesla turbine concept for ORC applications. Energy 2017;129:1055–62. http://dx.doi.org/10.1016/j.energy.2018.05.181.
[6] Song J, Gu C, wei Li, song X. Performance estimation of Tesla turbine applied in small scale Organic Rankine Cycle (ORC) system. Appl Therm Eng 2017;110:318–26. http://dx.doi.org/10.1016/j.applthermaleng.2016.08.168.
[7] Zhou Y, Zhu H, Li G, Ji F, Zhu X, Bao Y, Du F, Ding S, Zhao S. Investigation on performance and implementation of Tesla turbine in engine waste heat recovery. Energy Convers Manag 2019;179:326–38. http://dx.doi.org/10.1016/j.enconman.2018.10.071.
[8] Rice W. An analytica and experimental investigation of multiple-disk turbines. J Eng Power 1965;87:29–36. http://dx.doi.org/10.1115/1.3678134.
[9] Rice W. An analytical and experimental investigation of multiple-disk pumps and compressors. J Eng Power 1963;85:191–8. http://dx.doi.org/10.1115/1.3678134.
[10] Choon TW, Rahman AA, Jer FS, Aik LE. Optimization of Tesla turbine using computational fluid dynamics approach. In: 2011 IEEE symp. ind. electron. appl. ISIEA. 2011, p. 477–80. http://dx.doi.org/10.1109/ISIEA.2011.6108756.
[11] Song J, Ren X, dong Li, song X, Gu C, wei Zhang, ming M. One-dimensional model analysis and performance assessment of Tesla turbine. Appl Therm Eng 2018;134:546–54. http://dx.doi.org/10.1016/j.applthermaleng.2018.02.019.
[12] Alrabie M, Altamimi F, Altarrgemy M, Hadi F, Akbar MK. Method to design a hydro Tesla turbine for sensitivity to varying laminar Reynolds number modulated by changing working fluid viscosity. In: The ASME 11th int. conf. on energy sustainability. Three Park Avenue, New York, NY, USA: Amer Soc Mechanical Engineers; 2017, p. 10016–5990.
[13] Almeida ÁJ, Shahpari A, Vujicic Z, Sheikhnejad Y, Rodrigues F, Teixeira AL. Simplified model for power penalty when using PIN and APD receivers. Opt Commun 2017;392. http://dx.doi.org/10.1016/j.optcom.2017.01.025.
[14] Sheikhnejad Y, Ansari AB, Ferreira J, Martins N. Effects of parallel magnet bars and partially filled porous media on magneto-thermo-hydro-dynamic characteristics of pipe ferroconvection. Int J Heat Mass Transfer 2019;136:1273–81. http://dx.doi.org/10.1016/j.ijheatmasstransfer.2019.03.085.
[15] Sheikhnejad Y, Vujicic Z, Almeida ÁJ, Bastos R, Shahpari A, Teixeira AL. Analytical transient analysis of Peltier device for laser thermal tuning. In: Proceedings of SPIE - the international society for optical engineering. 2017, http://dx.doi.org/10.1117/12.2276372.
[16] Sheikhnejad Y, Bastos R, Vujicic Z, Shahpari A, Teixeira A. Laser thermal tuning by transient analytical analysis of peltier device. IEEE Photonics J 2017;9. http://dx.doi.org/10.1109/JPHOT.2017.2695522.
[17] Sheikhnejad Y, Hosseini R, Saffar Avval M. Experimental study on heat transfer enhancement of laminar ferrofluid flow in horizontal tube partially filled porous media under fixed parallel magnet bars. J Magn Magn Mater 2017;424. http://dx.doi.org/10.1016/j.jmmm.2016.09.098.
[18] Sheikhnejad Y, Mehrdad Hosseini M, Teixeira A, Shahpari A, Hosseini R, SaffarAvval M. Experimental investigation and three-dimensional numerical analysis of ferroconvection through horizontal tube under magnetic field of fixed parallel magnet bars. J Heat Transfer 2017;139. http://dx.doi.org/10.1115/1.4036620.
[19] Sheikhnejad Y, Hosseini R, Saffar-Avval M. Effect of different magnetic field distributions on laminar ferroconvection heat transfer in horizontal tube. J Magn Magn Mater 2015;389. http://dx.doi.org/10.1016/j.jmmm.2015.04.029.
[20] Sheikhnejad Y, Hosseini R, Avval MS. Laminar forced convection of ferrofluid in a horizontal tube partially filled with porous media in the presence of a magnetic field. J Porous Media 2015;18. http://dx.doi.org/10.1615/JPorMedia.v18.i4.60.
[21] Li R, Wang H, Yao E, Li M, Nan W. Experimental study on bladeless turbine using incompressible working medium. Adv Mech Eng 2017;9:1–12. http://dx.doi.org/10.1177/1687814016686935.